0026-895X/09/7503-542–554$20.00
MOLECULAR PHARMACOLOGY
Copyright © 2009 The American Society for Pharmacology and Experimental Therapeutics
Mol Pharmacol 75:542–554, 2009

Vol. 75, No. 3
51664/3436240
Printed in U.S.A.

Mechanisms and Functional Significance of Inhibition of Neuronal T-Type Calcium Channels by Isoflurane

Peihan Orestes, Damir Bojadzic, Robert M. Chow, and Slobodan M. Todorovic

Departments of Anesthesiology (P.O., D.B., R.M.C., S.M.T.) and Neuroscience (S.M.T.) and Neuroscience Graduate Program (P.O., S.M.T.), University of Virginia Health System, Charlottesville, Virginia

Received August 29, 2008; accepted November 26, 2008

ABSTRACT

Previous data have indicated that T-type calcium channels (low-voltage activated T-channels) are potently inhibited by volatile anesthetics. Although the interactions of T-channels with a number of anesthetics have been described, the mechanisms by which these agents modulate channel activity, and the functional consequences of such interactions, are not well studied. Here, we used patch-clamp recordings to explore the actions of a prototypical volatile anesthetic, isoflurane (Iso), on recombinant human $Ca_V3.1$ and $Ca_V3.2$ isoforms of T-channels. We also performed behavioral testing of anesthetic endpoints in mice lacking $Ca_V3.2$. Iso applied at resting channel states blocked current through both isoforms in a similar manner at clinically relevant concentrations (1 minimum alveolar concentration, MAC). Inhibition was more prominent at depolarized membrane potentials (−65 versus −100 mV) as evidenced by hyperpolarizing shifts in channel availability curves and a 2.5-fold decrease in IC_{50} values. Iso slowed recovery from inactivation and enhanced deactivation in both $Ca_V3.1$ and $Ca_V3.2$ in a comparable manner but caused a depolarizing shift in activation curves and greater use-dependent block of $Ca_V3.2$ channels. In behavioral tests, $Ca_V3.2$ knockout (KO) mice showed significantly decreased MAC in comparison with wild-type (WT) litter mates. KO and WT mice did not differ in loss of righting reflex, but mutant mice displayed a delayed onset of anesthetic induction. We conclude that state-dependent inhibition of T-channel isoforms in the central and peripheral nervous systems may contribute to isoflurane's important clinical effects.

The effects of general anesthetics on ion channels have been the subject of intense research since studies describing specific interactions between anesthetics and proteins (Franks and Lieb, 1982, 1994). It is now known that some ligand-gated channels (e.g., $GABA_A$), voltage-gated channels, and background potassium channels display anesthetic sensitivity in vitro that is within the concentration range achieved during general anesthesia (Franks, 2008). These channels have overlapping physiological roles and pharmacological profiles, making it difficult to assign aspects of the anesthetic state to individual channel types. Thus, it has become clear that further study of anesthetic mechanisms of action on specific ion channels is needed.

Low voltage-activated calcium channels activate with small depolarizations and allow calcium influx at resting potentials so that small differences in channel activity can result in large changes in cellular excitability and/or second-messenger pathways. Recent molecular studies have indicated that at least three isoforms of T-channels exist: $Ca_V3.1$ (α1G), $Ca_V3.2$ (α1H), and $Ca_V3.3$ (α1I) (Perez-Reyes, 2003). These channels are located throughout the spinothalamic pathway, in which nociceptive information passes from peripheral sensory neurons to the cortex. T-channels in small-sized dorsal root ganglia (DRG) neurons are believed to function in pain signaling (Todorovic and Lingle, 1998; Todorovic et al., 2001). Small and medium DRG neurons contain both $Ca_V3.1$ and $Ca_V3.2$ channels, although $Ca_V3.2$ predominates (Talley et al., 1999). $Ca_V3.2$-null mice have significantly decreased responses to acute somatic and visceral pain (Choi et al., 2007). Furthermore, oligonucleotide antisense studies against $Ca_V3.2$ reported similar results (Bourinet et al., 2005). This evidence makes it clear that T-channels are pronociceptive in the DRG.

In vivo studies have shown that anesthetic-induced loss of movement in response to pain is mediated primarily in the spinal cord. Actions in the brain are not apparently critical to

This work was supported by the National Institutes of Health National Institute of General Medical Sciences [Grant GM070726] and the National Institutes of Health National Institute of Neurological Disorders and Stroke [Grant F31-NS059190].

Article, publication date, and citation information can be found at http://molpharm.aspetjournals.org.

doi:10.1124/mol.108.051664.

ABBREVIATIONS: DRG, dorsal root ganglion; HVA (high-voltage-activated); Iso, isoflurane, 2-chloro-2-(difluoromethoxy)-1,1,1-trifluoro-ethane); Hal, halothane, 2-bromo-2-chloro-1,1,1-trifluoroethane; MAC, minimum alveolar concentration; LORR, loss of righting reflex; TTLORR, time to loss of righting reflex; KO, knockout; WT, wild type; HEK, human embryonic kidney; CNS, central nervous system.

inhibit motor responses to pain. This has been demonstrated in anesthetized rats, in which cervical transection of the spinal cord did not change the MAC for painful limb stimulation (Rampil, 1994). Furthermore, in situ studies have indicated that all three isoforms of T-channels are expressed predominantly in the dorsal horn of the spinal cord, an important pain processing region of CNS (Talley et al., 1999). Thus it is likely that any contributions of T-channels in the spinal cord to MAC of general anesthetics are indirect, because the effects would be on nociceptive pathways rather than on motor pathways in the spinal cord.

T-channels are also expressed in various brain regions and are particularly abundant in thalamic nuclei, where they are crucial for control of the functional states of those neurons (McCormick and Bal, 1997; Steriade, 2005). In particular, $Ca_V3.1$ is mainly expressed in thalamocortical relay neurons, whereas $Ca_V3.2$ and $Ca_V3.3$ are expressed in thalamic reticular neurons, the main inhibitory structure in the thalamus (Talley et al., 1999). Inhibition of thalamic processing of sensory information has been implicated recently as a possible contributor to clinical effects of anesthetics such as loss of consciousness and sedation (Alkire et al., 2000; Rudolph and Antkowiak, 2004; Franks, 2008). Therefore, the potential of T-channel isoforms expressed in the thalamus, spinal cord, and DRG as targets for the action of general anesthetics remains an important issue in our understanding of the cellular mechanisms of anesthetic action.

It has been shown previously that Iso at clinically relevant concentrations inhibits recombinant and native T-current variants in peripheral and central neurons (Study, 1994; Todorovic and Lingle, 1998; Ries and Puil, 1999; Todorovic et al., 2000; Joksovic et al., 2005a,b). Here, we studied the effects of clinically relevant concentrations of Iso on two kinetically similar isoforms of T-channels, $Ca_V3.1$ and $Ca_V3.2$, which are abundantly expressed in the thalamus, spinal cord, and DRG. By expressing T-type channels in a heterologous system, we are able to study individual isoforms without interference from other ionic conductances. Because it is known that Iso inhibits native T-channels, we now strive to describe the similarities and differences of its effects on each isoform and to compare in vivo effects of Iso on anesthetic endpoints in mice lacking these channels. This may lead to a better understanding of the distinct roles of these channels in anesthesia.

Materials and Methods

Human Embryonic Kidney-293 Cells. For recordings of recombinant T-currents, we used both transiently transfected and stably expressed $Ca_V3.1$ or $Ca_V3.2$ channels in human embryonic kidney (HEK-293) cells as reported previously (Joksovic et al., 2006). HEK-293 cells (CRL-1573; American Type Culture Collection, Manassas, VA) were grown in Dulbecco's modified Eagle's medium/F-12 media (Invitrogen, Carlsbad, CA) supplemented with 10% fetal bovine serum, penicillin G (100 mg/ml), and streptomycin (0.1 mg/ml). Transiently transfected cell lines were made using cDNA encoding human $Ca_V3.1$ or $Ca_V3.2$, and a plasmid encoding the CD8 antigen. Cells were then incubated with polystyrene microbeads coated with CD8 antibody (Dynabeads M-450 CD8; Dynal GmbH, Hamburg, Germany). After ~48 h, cells with microbeads bound were selected for electrophysiology.

In Vitro Anesthetic Preparation. Isoflurane (Abbott Laboratories, Abbott Park, IL) was prepared as a saturated stock solution incubated overnight in a tightly sealed glass bottle (40 ml of Iso and 60 ml of external solution) and freshly diluted to appropriate concentrations at the time of experiments, using only the upper aqueous layer. To quantify the actual anesthetic concentrations in solutions, we had analyzed previously samples of identically prepared saturated stock solutions and aliquots in a gas chromatograph calibrated with appropriate volatile anesthetic standards (Todorovic and Lingle, 1998; Joksovic et al., 2005b). By measuring actual concentrations, we found less than 10% loss if the solution was used within 30 min after preparation. Test solutions were maintained in tightly sealed, all-glass syringes.

Electrophysiology. All recordings were made using standard whole-cell techniques. Electrodes were fabricated from borosilicate microcapillary tubes (Drummond Scientific, Broomall, PA) and fire-polished to final resistances of 2 to 3 MΩ. Voltage commands and digitization of membrane voltages and currents were done with Clampex 9.2 of the pClamp software package (Molecular Devices, Sunnyvale, CA), running on an IBM-compatible computer. Membrane voltages and currents were recorded with an Axopatch 200B patch-clamp amplifier (Molecular Devices). Data were analyzed using Clampfit 9.2 (Molecular Devices) and Origin 7.0 (OriginLab Corp, Northampton, MA). Currents were filtered at 2 kHz. Series resistance (R_s) and membrane capacitance (C_m) values were taken directly from readings on the amplifier after electronic subtraction of the capacitative transients. We compensated for 50 to 80% of R_s. Cells were held (V_h) at −90 mV and depolarized to a test potential (V_t) of −30 mV every 10 to 20 s to evoke inward Ba^{2+} currents unless otherwise noted. In most experiments, a P/N protocol was used for online leak subtraction.

Multiple independently controlled glass syringes served as reservoirs for a gravity-driven local perfusion system, in which manually controlled valves allowed for switching between syringes. Solution exchange was accomplished by constant suction through a glass capillary tube at the opposite end of the recording dish. All drugs were prepared as stock solutions and freshly diluted to appropriate concentrations at the time of experiments. The external recording solution used to isolate Ba^{2+} currents in HEK-293 cells contained 2 to 10 mM $BaCl_2$, 152 mM tetraethylammonium chloride, and 10 mM HEPES, pH adjusted to 7.4 with tetraethylammonium-OH. The internal solution contained 110 mM cesium-methane sulfonate, 14 mM phosphocreatine, 40 mM HEPES, 2 mM Mg-ATP, and 0.1 mM Na-GTP, adjusted to pH 7.2 with KOH.

Data Analysis and Statistical Procedures. Peak currents and exponential fits to currents were calculated using Clampfit, whereas curve-fitting was performed using Origin 7 software. For general statistical evaluations, we used one- and two-way analyses of variance with values <0.05 judged to be statistically significant and paired or unpaired Student's t tests as appropriate.

Analysis of Current Blockade. The percentage reduction in peak T-current at a given Iso concentration was used to generate concentration-response curves. For each such curve, all points are averages of multiple determinations obtained from at least three different cells. In most of the cells, we tested at least two different concentrations of Iso. On all plots, vertical bars indicate ± S.E.M. Mean values on concentration-response curves were fit to the following equation: $PB([\text{Iso}]) = PB_{max}/(1 + (IC_{50}/[\text{Iso}])^{n_H})$, where PB_{max} is the maximal percent block of peak T-current, IC_{50} is the concentration that produces 50% of maximal inhibition, and n_H is the apparent Hill coefficient for blockade. Fitted values are typically reported with 95% linear confidence limits.

Analysis of Current. The voltage dependence of steady-state activation was described with a single Boltzmann distribution: $G(V) = G_{max}/(1 + \exp[-(V - V_{50})/k])$, where G_{max} is the maximal estimated conductance, V_{50} is the half-maximal voltage, and k (units of millivolts) represents the voltage dependence of the distribution. The voltage-dependence of steady-state inactivation was described with a single Boltzmann distribution: $I(V) = I_{max}/(1 + \exp[(V - V_{50})/k])$, where I_{max} is the maximal current, V_{50} is the half-maximal

voltage, and k (units of millivolts) represents the voltage dependence of the distribution.

The time courses of macroscopic current inactivation and deactivation of tail currents were fitted using a single exponential equation: $f(t) = A_1\exp(-t/\tau_1)$, yielding one time constant (τ_1) and its amplitude (A_1). For fitting the time course of recovery from inactivation, a double exponential function was used, yielding two time constants (τ_1 and τ_2) and their corresponding amplitudes (A_1 and A_2). For all steady-state inactivation curves, fitted values typically were reported with 95% linear confidence limits.

Behavioral Studies. Adult mice of either gender were used for all behavioral studies. $Ca_V3.2$ knockout mice [$Ca_V3.2(-/-)$] and their age-matched WT litter mates [$Ca_V3.2(+/+)$] were studied at 16 to 60 weeks of age. The initial breeding pair for our colony of $Ca_V3.2(-/-)$ mice was obtained through the courtesy of Dr. Kevin Campbell (University of Iowa, Iowa City, IA). These mice were repeatedly backcrossed for at least six generations against wild-type (C57BL/65J) mice. Animals were genotyped using tail biopsy. All behavioral experiments were performed in a blinded manner. Mutant mice were normal in appearance, weight, and overt behavior. They demonstrated a brisk righting reflex and in a previous study showed no differences in motor abilities under control conditions (Choi et al., 2007).

To compare anesthetic phenotypes accurately, we used procedures similar to those used recently to characterize $Ca_V3.1$-deficient mice for behavioral testing of anesthetic endpoints (Petrenko et al., 2007). Animals were tested individually in a small Plexiglas chamber that was connected to an anesthetic vaporizer via a plastic nose cone made from latex glove. Iso was vaporized in 2 to 6 l/min oxygen. Anesthetic concentration was constantly monitored by an infrared gas analyzer (Datex-Engtstrom, Helsinki, Finland). Each concentration of Iso was maintained for a minimum equilibration period of 20 min. In all behavioral experiments, we recorded rectal temperatures (Oakton Instruments, Vernon Hills, IL) before and after each measurement. Body temperature was actively maintained between 36° and 38°C with an electric heat mat placed beneath the testing chamber.

We used loss of righting reflex (LORR) as a measure of anesthetic-induced hypnosis. An initial concentration of 0.6% atm Iso was administered and allowed to equilibrate. The chamber was then rotated to gently place the mouse on its back, and the mouse was monitored for 3 consecutive tries, the first lasting 45 s, and the second two lasting 1 min each. LORR onset was considered to be a failure of the animal to right itself on all three tries but disregarded if the animal was able to right itself on any of the three. None of the animals demonstrated LORR at this concentration. Iso concentration was then increased by 0.1% atm for another equilibration period, and the response was tested again. LORR ED_{50} (50% concentration for LORR) was calculated by averaging the two concentrations at which the mouse either retained or lost its righting reflex.

Time to LORR (TTLORR) was used as another measure of Iso hypnosis. We measured the ability of mice to right themselves within 15 s after being placed on their backs. Mice were evaluated at 30-s intervals after beginning exposure to 1.0, 1.4, or 2.0% Iso. The average time to first LORR (over three trials) was considered time to LORR. We also determined time to LORR for the intravenous anesthetic 2,6 diisopropylphenol (propofol; AstraZeneca Pharmaceuticals, Wilmington, DE), which was given intraperitoneally (180 mg/kg) after a negative aspiration test. The TTLORR after propofol injections was assessed by using two consecutive 15-s periods every minute or when deemed necessary by observation. Failure of the mouse to right itself in both constituted the onset of the LORR.

The immobilizing properties of Iso or halothane (Hal) were examined using tail-clamp experiments to determine MAC. The volatile anesthetics were delivered to the mice through a modified thumb portion of a latex glove. A latex glove was used to ensure that the mice were being exposed to a constant concentration of volatile anesthetic. The glove tip was connected to a vaporizer and an oxygen source with a flow of 2 l/min. For Iso, the concentration started at 0.9% for KO mice and 1.1% for the control mice with incremental increases of 0.1%. This experiment was repeated with Hal starting at an initial concentration of 0.8% for KO mice and 1.0% for control mice with incremental increases of 0.1%. These values were established after initial testing of both knockouts and controls. The mice were equilibrated at each concentration of anesthetic for at least 30 min (Iso) or 40 min (Hal). A plastic clamp was then used to clamp the proximal third of the mouse's tail. If a response was elicited, the concentration of anesthetic was subsequently increased by 0.1%. If there was no response, a metal artery clamp was clamped on the proximal third of the tail on its first notch. Then, if a response was elicited, the concentration was increased. However, if there was still no response, then this concentration was recorded as the value at which the mouse had no response. This is because the metal artery clamp is a suprathreshold stimulus. MAC was calculated by averaging the two concentrations at which the mouse either retained or lost the movement response. If the same mice were used for LORR and MAC studies, at least 1 week was allowed between each treatment for recovery. For behavioral studies, statistical analysis was performed using Student's t test or Mann-Whitney rank sum test.

Animals. Ethical approval was obtained for all experimental protocols from the University of Virginia Animal Care and Use Committee (Charlottesville, VA). All experiments were conducted in accordance with the Guide for the Care and Use of Laboratory Animals adopted by the U.S. National Institutes of Health. Every effort was made to minimize animal suffering and the number of animals used.

Results

State-Dependent Inhibition of T-Current Variants by Isoflurane. We first characterized the effects of 300 and 600 μM Iso on $Ca_V3.1$ and $Ca_V3.2$ currents in the form of a current-voltage (I-V) series. Most notable in Fig. 1, A and B, are the concentration-dependent and almost complete inhibition of current amplitude over the wide range of test potentials for both isoforms. When normalized peak current was converted to conductance, it is noticeable that 300 μM Iso produced a significant (~4 mV) depolarizing shift in the conductance curves of $Ca_V3.2$, although it had a minimal effect on $Ca_V3.1$ (Fig. 1C). Based on these initial results, we further explored the differential effects of Iso on these two key isoforms of human T-channels. We chose to perform our other studies using 300 μM Iso, a clinically relevant concentration for in vitro studies (MAC, ~320 μM) (Franks and Lieb, 1994).

Inactivation is one of the main features that distinguishes T-currents from high voltage-activated currents. Inactivation of T-currents is normally complete with voltage-clamp commands that are subthreshold for high-voltage activation. It is noteworthy that alteration of T-current inactivation kinetics by anesthetic agents can result in very different operational ranges of membrane potential in which action potential firing can be generated. Thus, we analyzed macroscopic inactivation kinetics of current waveforms fitted with a single exponential function (Fig. 2A). Iso (300 μM) minimally affected macroscopic current inactivation in both isoforms as evidenced by largely overlapping points before (open symbols) and after Iso application (filled symbols). Next, we assessed the influence of the same concentration of Iso on macroscopic current activation by measuring 10 to 90% rise time. Figure 2B shows that Iso at 300 μM has very little effect on 10 to 90% rise times for either $Ca_V3.1$ or $Ca_V3.2$. Solid curves denote single exponential equation fits. However, 600 μM Iso

significantly increased the rate of macroscopic current activation and inactivation (data not shown). On average, for $Ca_V3.1$ constructs, 10 to 90% rise time (V_h −90 mV; V_t −30 mV) was in control conditions 4.3 ± 0.3 ms and during Iso application, 3.0 ± 0.4 ms ($n = 8$, $p < 0.01$), whereas for $Ca_V3.2$ constructs, it was 4.7 ± 0.4 ms in control ($n = 6$) and 3.4 ± 0.1 ms with Iso ($n = 9$, $p < 0.05$). Likewise, average inactivation time constants for $Ca_V3.1$ constructs in these cells (V_h −90 mV; V_t −30 mV) was in control conditions 15.3 ± 1.2 ms and during Iso application, 10.6 ± 0.9 ms ($p < 0.001$), whereas for $Ca_V3.2$ constructs, it was 21.2 ± 0.9 ms in control and 12.2 ± 0.9 ms with Iso ($p < 0.001$).

T-channels deactivate (close) much more slowly than other voltage-gated Ca^{2+} channels. That is, they take more time to return from the open state to the resting state. This is evidenced by a slowly relaxing tail current at the end of short-

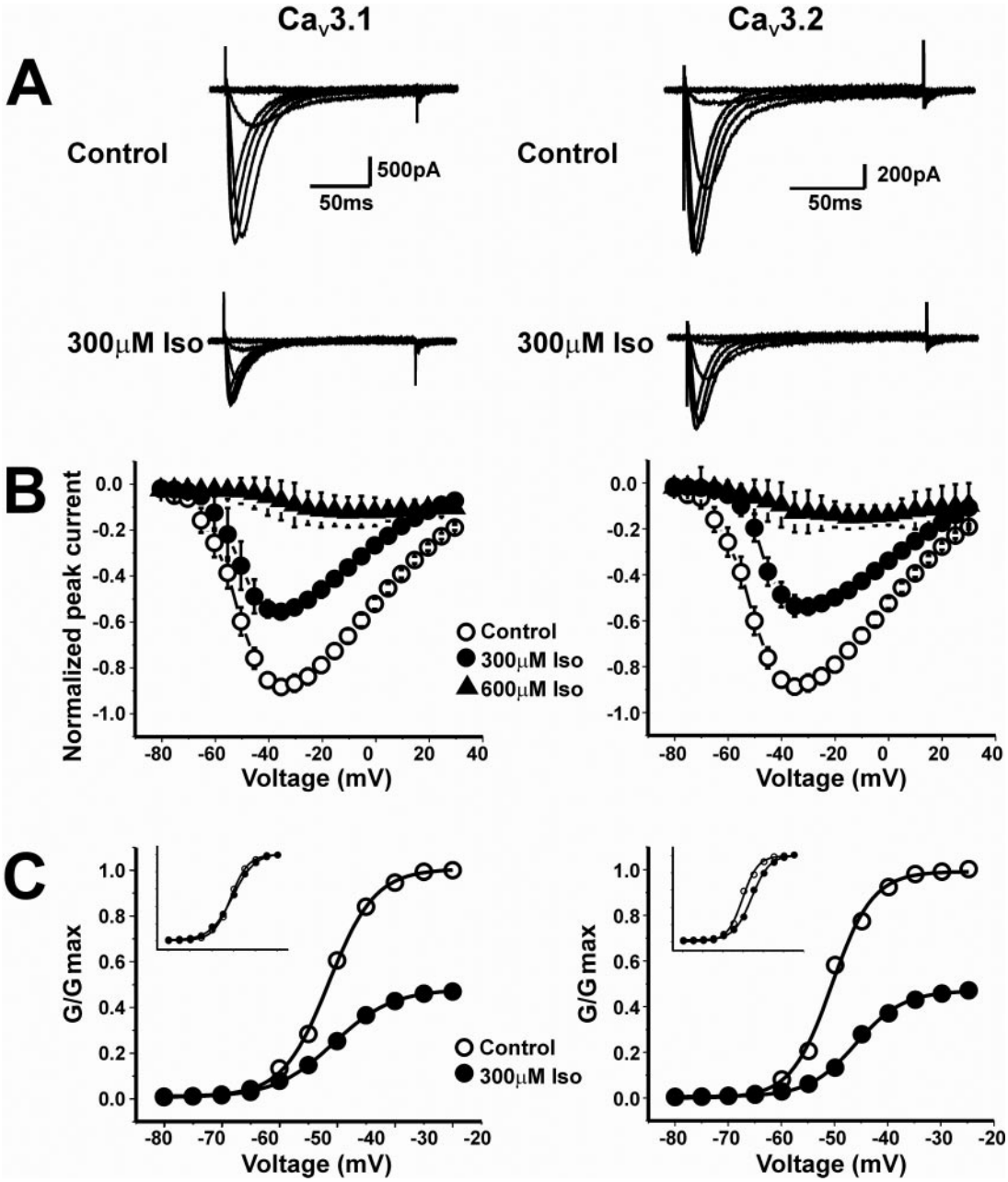

Fig. 1. A, families of representative traces from current-voltage series traces from HEK cells transfected with $Ca_V3.1$ (left) and $Ca_V3.2$ (right) constructs. Cells were held at −90 mV, with steps ranging from −80 to −20 mV before (control, top traces) and during application of 300 μM Iso (bottom traces). Traces are shown in 10-mV increments for clarity. B, average normalized current-voltage relationships in the same cells ($n = 6–8$) before (○) and during application of 300 μM Iso (●) and 600 μM Iso (▲) for $Ca_V3.1$ (left) and $Ca_V3.2$ (right) constructs. Note that Iso blocked inward currents of both isoforms over the wide range of test potentials. Vertical lines represent S.E.M. and are visible only if larger than symbols. C, apparent peak conductance values calculated from I-V curves in B plotted against command potentials. The extrapolated reversal potential (E_r) was taken to be +55 mV. The estimates of V_{50} and k show only small shifts with even up to 20-mV differences in assumed reversal potential values. Changes in conductance in control conditions (open symbols) and during applications of 300 μM Iso (filled symbols) are presented with midpoints (V_{50}) and slope (k) from fitted data (solid lines) using a Boltzmann equation giving the following values: $Ca_V3.1$ control: V_{50}, −51.4 ± 0.1 mV; k, 4.0 ± 0.1 mV; $Ca_V3.1$ Iso: V_{50}, −50.6 ± 0.2 mV; k, 5.1 ± 0.2 mV; $Ca_V3.2$ control: V_{50}, −50.6 ± 0.3 mV; k, 3.8 ± 0.2 mV; $Ca_V3.2$ Iso: V_{50}, −46.1 ± 0.3 mV; k, 4.4 ± 0.3 mV. Inset, same data are normalized to peak conductance.

activating test pulse. This transition determines the mean open time and the bursting behavior of the channel. Hence, to study the possible effects of Iso on the voltage-dependence of deactivation kinetics, tail currents were recorded over a sufficiently negative range of membrane potentials (e.g., −160 to −70 mV in 10-mV increments), after an 8-ms depolarizing step to −30 mV (Todorovic and Lingle, 1998). We determined the time constant of current decay using a single exponential fit of the time course of tail currents before and during application of 300 μM Iso in the same cells (Fig. 3A). As shown in Fig. 3B, 300 μM Iso markedly speeds deactivation time constants in both $Ca_V3.1$ and $Ca_V3.2$ isoforms over a wide range of membrane potentials. These changes were significant at all voltages shown (paired t test, $p < 0.05$) but are most impressive at physiologically relevant voltages (e.g., 2–3-fold change at −70 mV). This is important because deactivation can become physiologically significant after brief depolarizations that activate T-channels. The driving force for ion permeation at deactivation potentials is large so that significant Ca^{2+} entry can occur until the channels are completely deactivated. Thus, T-currents may serve to promote Ca^{2+} influx during the repolarization phase of action potentials in neurons (McCobb and Beam, 1991). Furthermore, by changing the time constant and/or voltage-dependence of T-current deactivation, anesthetic agents can modulate neuronal excitability.

Binding to inactivated states is an important property of drugs that modulate ion channels because it can provide selectivity to their action. Transitions from closed to inactivated states can be measured using long prepulses at different potentials, producing what are commonly referred to as the steady-state inactivation curves. Steady-state inactivation curves were assessed using a standard double-pulse protocol with 3.6-s long prepulses to variable voltages (from −110 to −45 mV) and test potentials to −40 mV. Figure 4A shows representative traces of currents in HEK cells transfected with $Ca_V3.1$ (left) and $Ca_V3.2$ (right) constructs before (top) and after application of 300 μM Iso (bottom). Iso (60, 150 and 300 μM) caused concentration-dependent hyperpolarizing shifts of steady-state relationships even after exposure to as little as 60 μM Iso (Fig. 4B, top, left). Applications of 300 μM Iso resulted in approximately 6-mV leftward shift on $Ca_V3.1$ and approximately 4-mV shift on $Ca_V3.2$ (Fig. 4B, bottom). All changes were statistically significant ($p < 0.05$), except for the effects of 60 μM Iso on $Ca_V3.2$ (paired t test, $p > 0.05$).

These data suggest that Iso binds to and stabilizes inactive states of the channel and thus is a more potent blocker at depolarized membrane potentials. To further confirm this notion, we evaluated concentration-response curves for Iso inhibition of T-currents at different holding potentials. Cells were exposed to the same concentrations of Iso while held at membrane potentials of −100 and −65 mV. Representative traces (Fig. 5, A and B) illustrate a 2- to 3-fold greater block of peak $Ca_V3.1$ and $Ca_V3.2$ current when cells were held at −65 mV rather than −100 mV. Figure 5C shows the average

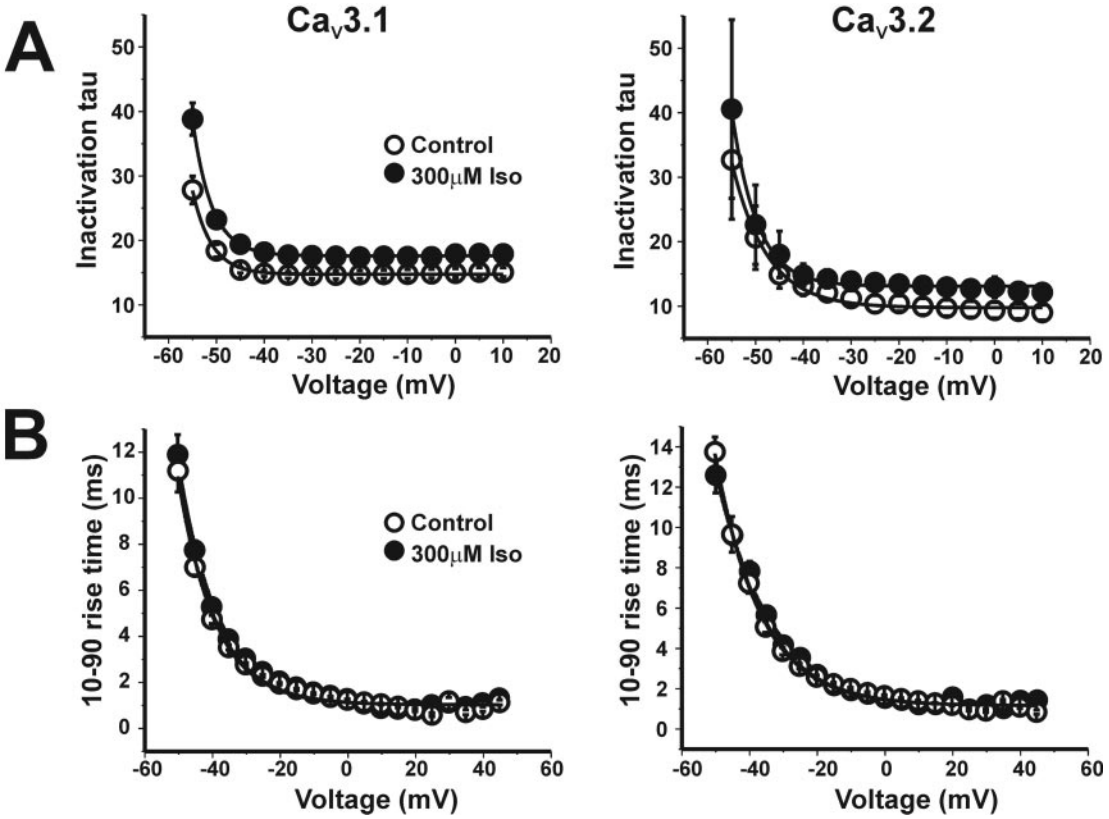

Fig. 2. A, rates of macroscopic current inactivation ($n = 6–8$, error bars represent S.E.M.) from the same cells used to generate current-voltage curves depicted in Fig. 1 in control (open symbols) and during application of 300 μM Iso (filled symbols) for $Ca_V3.1$ (left) and $Ca_V3.2$ (right). All points represent averages from multiple cells where inactivation τ was obtained at indicated potentials by fitting the decaying portion of the current with a single exponential function. B, all points represent averages of 10 to 90 rise time of the same cells. Rise time was measured as time between 10 and 90% of peak current. Solid lines are fits by a single exponential function. Calculated τ values were as follows: $Ca_V3.1$ control, 11.0 ± 0.5; $Ca_V3.1$ Iso, 11.5 ± 0.4; $Ca_V3.2$ control, 13.5 ± 0.4; $Ca_V3.2$ Iso, 15.8 ± 0.6 ($n = 6–8$, error bars represent S.E.M.).

concentration-response data from multiple cells. Depolarizing the cells decreased the IC_{50} value of Iso approximately 2-fold for $Ca_V3.1$ (left) and 2.7-fold for $Ca_V3.2$ (right). As result, the difference in the degree of inhibition of peak current at 300 μM Iso is significant for both isoforms at different holding potentials (*t* test, $p < 0.05$).

T-channels can recover from inactivation during sufficiently long hyperpolarizations of the neuronal membrane caused by inhibitory synaptic potentials in CNS (Perez-Reyes, 2003) or the effects of neuromodulators like serotonin in peripheral sensory neurons (Nelson et al., 2005). Rates of recovery can drastically influence firing properties of cells that express T-channels. Thus, we determined the effect of Iso on recovery from inactivation (deinactivation) of T-channels using our standard double-pulse protocol with variable duration prepulse (Fig. 6A). As expected from the effects of Iso on steady-state inactivation (Fig. 4), recovery from inactivation was slowed in both $Ca_V3.1$ and $Ca_V3.2$ after exposure to 300 μM Iso (Fig. 6, A and B). Average data in Fig. 6B indicate that, when fitted with a double exponential curve, Iso produced a 1.5-fold increase in both isoforms of the slow component of the time constant and in $Ca_V3.1$'s fast component. It is interesting that Iso caused a 3-fold increase of $Ca_V3.2$'s fast component.

To further explore the mechanism of Iso inhibition of these channels, we investigated the tonic blockade of the channel by using a protocol that allowed the assessment of Iso interaction with resting states of the channel. First, we obtained baseline measurements of peak current amplitude when cells were repeatedly depolarized to −30 mV every 10 s, then applied 300 μM Iso to cells for 2 min with no stimulation, and finally measured the amplitude of the first current wave form after resuming stimulation after Iso application (Fig. 7, A and B). A summary histogram comparing current amplitudes after the first depolarizing pulse with normal inhibition shows that there is a similar degree of block of the channel in

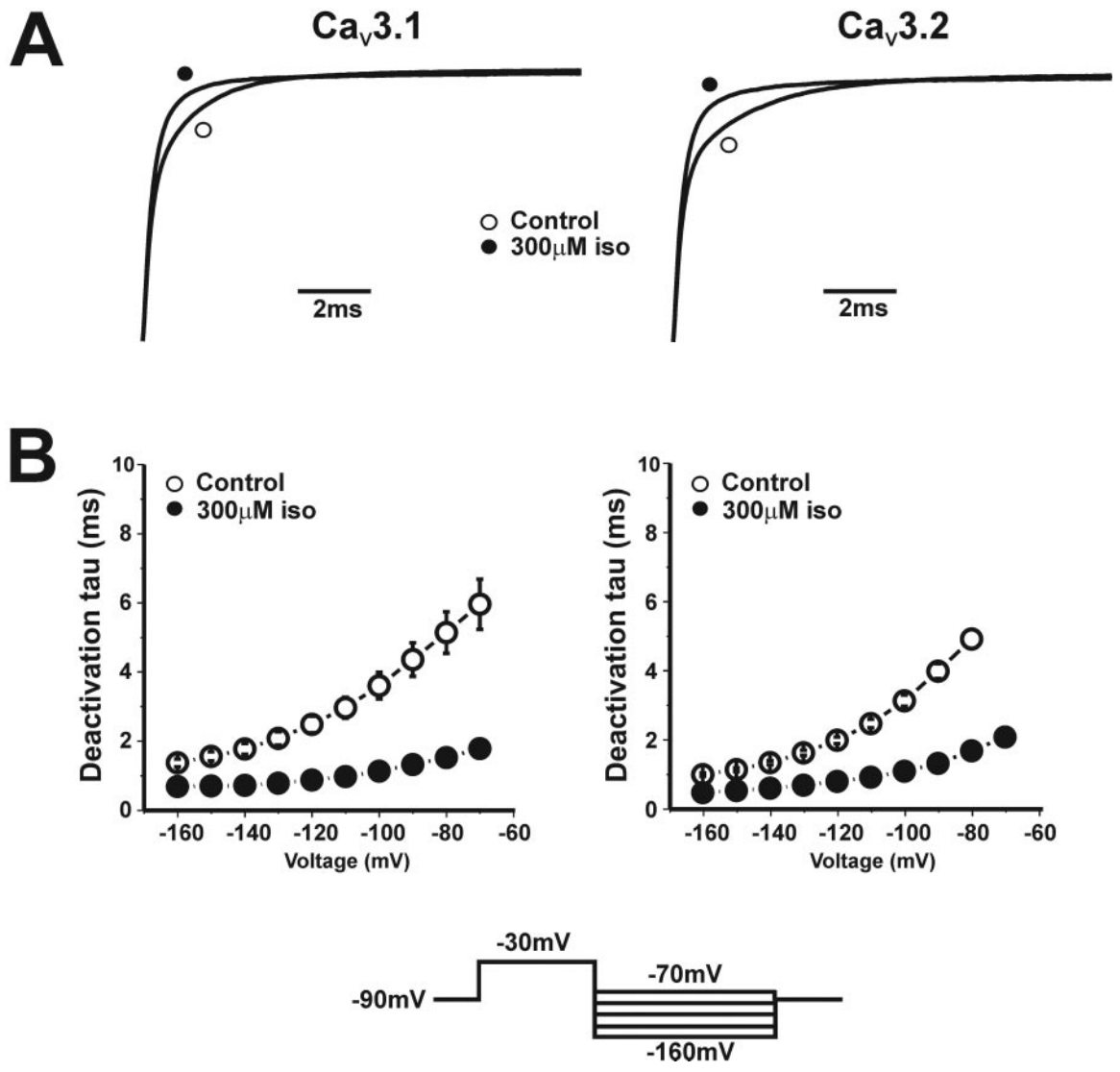

Fig. 3. Isoflurane (300 μM) increases the speed of current deactivation in both $Ca_V3.1$ (left) and $Ca_V3.2$ (right) constructs. A, normalized traces of tail currents from representative cells at deactivating test potentials of −70 mV for Iso (top traces) and control (bottom traces). B, deactivating tail currents in control (open symbols) and during application of 300 μM Iso (filled symbols) were fit with a single exponential function, and the resulting τ values are plotted ($n = 5$, error bars represent S.E.M.). All points are statistically significant ($p < 0.05$). Insert at the bottom depicts the protocol used in these experiments, where cells were held at −90 mV, then subjected to a 8-ms long activating pulse to −30 mV, and followed by variable deactivating steps from −160 to −70 mV.

both isoforms: ~57% block of the resting (previously non-stimulated) channels versus ~50% of the constantly stimulated channels. Thus, it seems that Iso binds preferentially to resting states over open and inactive channel states.

Some blockers more effectively inhibit currents when channels are more frequently depolarized, presumably due to greater access to high-affinity binding states. As shown in Fig. 8A, 300 μM Iso blocked ~50% of $Ca_V3.1$ current when cells were stimulated every 6 s. When the stimulation frequency was reduced to once every 60s, only ~40% inhibition was observed ($p > 0.05$). A greater difference is seen in $Ca_V3.2$ as depicted by representative current traces and time course of current inhibition (Fig. 8B). Histograms shown in Fig. 8C indicate that the same concentration of Iso inhibits ~70% of $Ca_V3.2$ current when stimulated every 6 s and only ~50% when stimulated every 60 s (paired t test, $p < 0.05$). This use-dependence of inhibition indicates that Iso also binds to channel states entered upon membrane depolarization.

Mice Lacking $Ca_V3.2$ Have Altered Sensitivity to Volatile Anesthetics. A complete anesthetic state involves loss of consciousness (hypnosis), movement (immobilization), pain sensation (analgesia), and recollection of the event (amnesia). New theories propose that multiple endpoints of anesthesia are mediated by multiple relevant cellular mechanisms (Urban, 2002; Rudolph and Antkowiak, 2004). According to this multisite hypothesis, the importance of a particular molecular target depends on the specific anesthetic and the specific endpoint in consideration. In agreement with this view, recent genetic studies with knockout mice of various ion channels have demonstrated variable, often small, alterations only in certain endpoints of anesthetic states (Rudolph and Antkowiak, 2004; Franks, 2008). Calcium current inhibition may be important to anesthetic action in either of two ways. First, it is possible that selective inhibition of particular Ca^{2+} channel subtypes in CNS neurons may be central to the effects of some

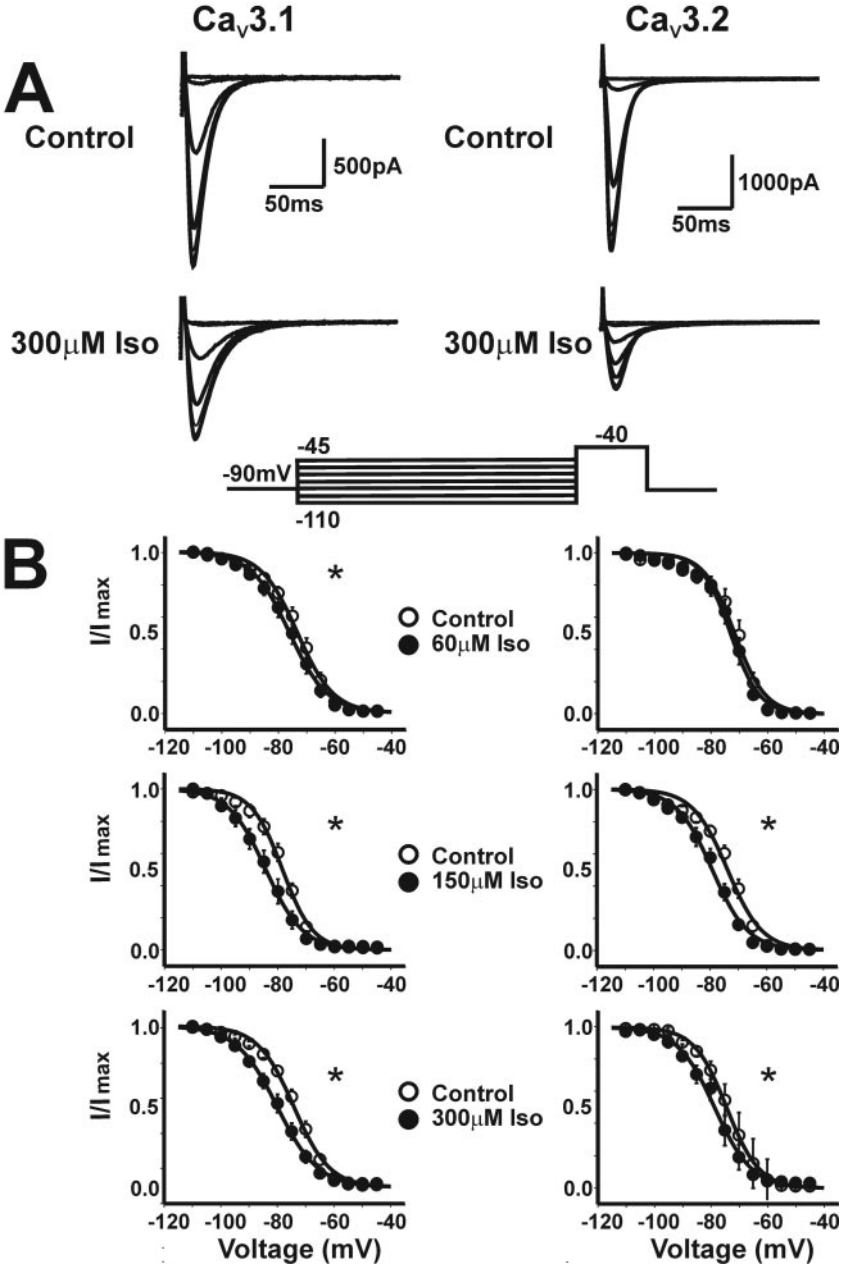

Fig. 4. Steady-state inactivation in human $Ca_V3.1$ (left) and $Ca_V3.2$ Ca^{2+} (right) channels. A, representative current traces are shown in control (top) and during application of 300 μM Iso (bottom) every 10 mV for clarity. Voltage protocol is depicted at the bottom: currents were measured using 3.6-s long inactivating pulses (−110 to −45 mV), followed by a brief activating step to −40 mV. B, average data from similar experiments with different concentrations of Iso were fitted with Boltzmann equation (solid lines) giving V_{50} (midpoint of inactivation) and slope (k) of the curve (n = 4–13 cells, error bars represent S.E.M.). Left, $Ca_V3.1$ (top): control, V_{50}, −73.2 ± 0.4 mV; k, 6.4 ± 0.3 mV; 60 μM Iso: V_{50}, −76.1 ± 0.4 mV; k, 6.8 ± 0.3 mV. Middle, control: V_{50}, −78.5 ± 0.3 mV; k 5.4 ± 0.3 mV; 150 μM Iso: V_{50}, −84.3 ± 0.3 mV; k, 6.6 ± 0.3 mV. Bottom, control: V_{50}, −74.2 ± 0.3 mV; k, 6.3 ± 0.2 mV; 300 μM Iso: V_{50}, −80.1 ± 0.3 mV; k, 7.2 ± 0.3 mV. Right, $Ca_V3.2$ (top): control, V_{50}, −71.7 ± 0.5 mV; k, 5.4 ± 0.5; 60 μM Iso, V_{50}, −72.7 ± 0.7 mV; k, 5.4 ± 0.6 mV. Middle, control: V_{50}, −73.7 ± 0.6 mV; k, 6.1 ± 0.5 mV; 150 μM Iso: V_{50}, −78.6 ± 0.6 mV; k, 6.0 ± 0.6 mV. Bottom, control: V_{50}, −74.3 ± 0.3 mV; k, 5.7 ± 0.3 mV; 300 μM Iso: V_{50}, −78.6 ± 0.3 mV; k, 6.6 ± 0.3 mV. *, significance by paired t test ($p < 0.05$).

general anesthetics. Second, there are large differences in the quality of the anesthetic state induced by different agents. Differential effects of volatile anesthetics on Ca^{2+} channels versus other potential targets may contribute to the diversity of effects produced by these agents. Thus, we tested the anesthetic sensitivity of mice lacking $Ca_V3.2$ channels and compared the results with findings reported recently regarding the $Ca_V3.1$ isoform (Petrenko et al., 2007).

First we examined the immobilizing effects of Iso in mutant and wild-type litter mate mice using tail-clamp tests for the determination of MAC. Figure 9A shows that $Ca_V3.2$ knockout mice have approximately 15% decreased MAC requirements for Iso and Hal (Mann-Whitney rank sum test, $p < 0.001$). In contrast, KO mice show no statistical difference from wild-type litter mates for the concentration of Iso needed to reach LORR (Fig. 9B). However, mutant mice have a considerably slower induction of anesthesia as manifested by approximately 60% longer times for loss of righting reflex (TTLORR) at 1.0 and 1.4% ($p < 0.05$, t test) but not with 2% Iso (Fig. 9C). It seems that slower anesthetic induction was isoflurane-specific because we did not observe difference in TTLORR between the wild-type and mutant mice after intraperitoneal injections of a prototypical intravenous anesthetic, propofol, at 180 mg/kg ($n = 13$ in each group, $p > 0.05$, Mann-Whitney rank sum test; data not shown).

Discussion

Biophysical Mechanisms of T-Channel Inhibition by Isoflurane. Recent studies have indicated that among other native voltage-gated calcium channels, T-channels are particularly sensitive to inhibition by volatile anesthetics (Takenoshita and Steinbach, 1991; Herrington and Lingle, 1992; Study, 1994; McDowell et al., 1996; Todorovic and Lingle, 1998; Ries and Puil, 1999; Joksovic et al., 2005a,b). This study describes the inhibition of cloned human $Ca_V3.1$ and $Ca_V3.2$ T-type channels by a commonly used volatile anesthetic, isoflurane. Previous pharmacological studies have demonstrated a similar sensitivity of recombinant rat $Ca_V3.1$ (Todorovic et al., 2000) and rat $Ca_V3.3$ (Joksovic et al., 2005a) to this anesthetic but have not presented an in-depth com-

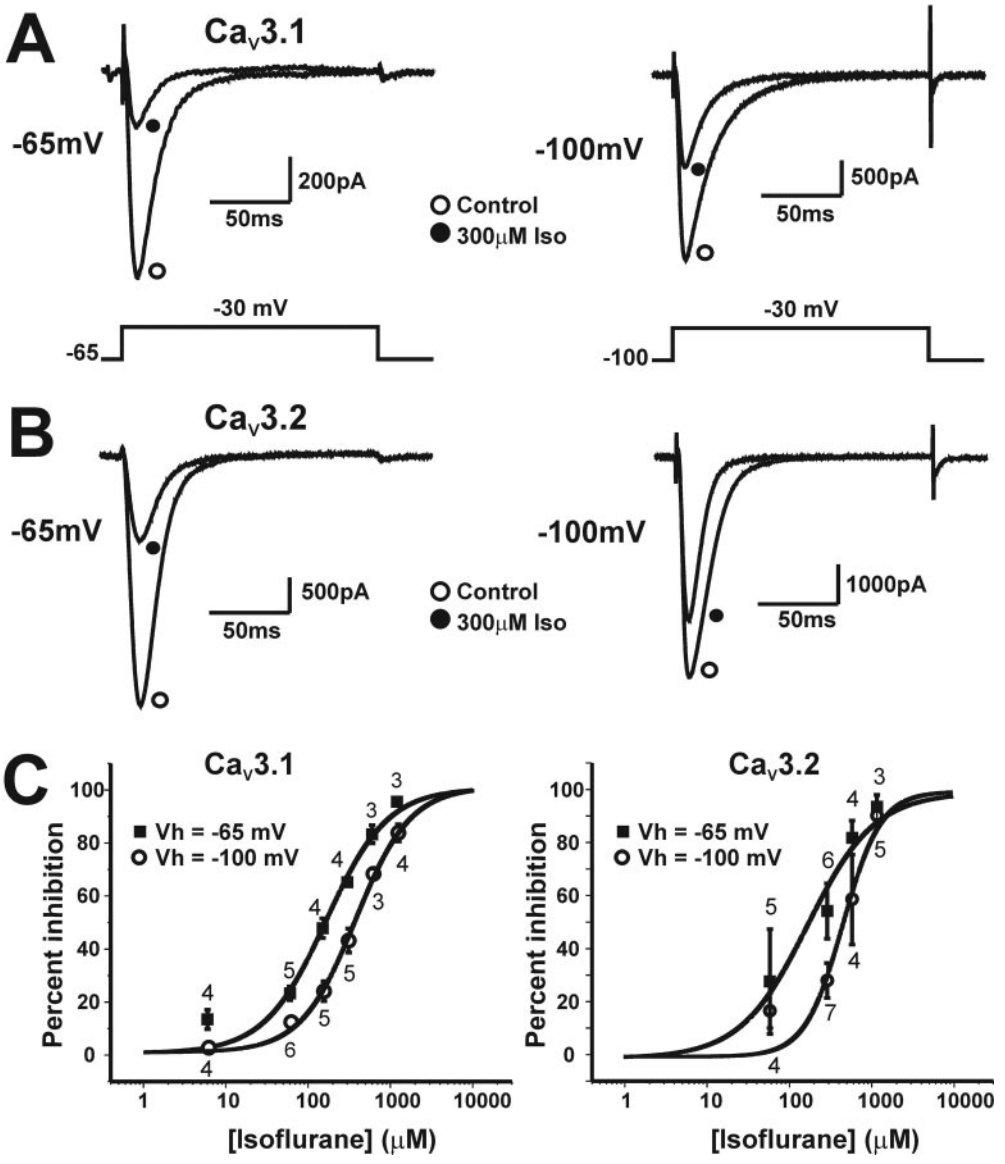

Fig. 5. Voltage-dependent inhibition of human T-channel isoforms by isoflurane. A, representative traces of inward currents in the absence and presence of 300 μM Iso recorded from $Ca_V3.1$ in response to voltage steps to V_t −30 mV from holding potentials (V_h) of −65 (left) or −100 mV (right) applied every 10 s. In this cell, Iso inhibited approximately 50% of $Ca_V3.1$ current at V_h −100 mV and more than 70% at V_h −65 mV. B, A similar effect is evident for $Ca_V3.2$ because Iso inhibited (in the same cell) only approximately 25% current at V_h −100 mV and approximately 66% at V_h −65 mV. Voltage protocols are depicted at the bottom shown in A and B. C, percentage of inhibition of peak current is plotted against drug concentration. IC_{50} values from fitted data (solid lines) using a Hill equation were the following: $Ca_V3.1$ at V_h −65 mV, 166 ± 20 μM; slope, 1.2 ± 0.2; $Ca_V3.1$ at V_h −100 mV, 363 ± 13 μM; slope, 1.3 ± 0.1; $Ca_V3.2$ at V_h −65 mV, 172 ± 43 μM; slope, 1.1 ± 0.3; $Ca_V3.2$ at V_h −100 mV, 464 ± 85 μM; slope, 1.9 ± 0.7. Number of cells recorded for each point is indicated on the graph. Error bars indicate S.E.M.

parison between isoforms. In this article, we did not examine $Ca_V3.3$, choosing to focus on the two more kinetically similar but differentially tissue-expressed isoforms. For greatest relevance to human application, we performed all experiments using clinically pertinent anesthetic concentrations and used human isoforms of recombinant channels.

Our results strongly suggest that Iso inhibition of $Ca_V3.1$ and $Ca_V3.2$ T-currents occur primarily by interaction with resting channel states because we observed significant tonic channel inhibition. However, functionally important state-dependent features of Iso inhibition of T-currents occur via stabilization of inactive channel states. This is seen in hyperpolarizing shifts in steady-state inactivation curves, greater potency of inhibition at more depolarized holding potentials, and slowing of recovery from inactivation. Evidence also points to Iso binding to open channels. Iso inhibited gating of $Ca_V3.2$ as evidenced by a depolarizing shift in channel activation curves in I-V relationships. Channel deactivation determines channel open time and bursting behavior. Thus, the observation that Iso allows both $Ca_V3.1$ and $Ca_V3.2$ channels to close more rapidly suggests an interaction with activation gate closure after repolarization. In addition, Iso inhibition of $Ca_V3.2$ T-current increases with more frequent channel openings. This use-dependent block provides additional evidence that the Iso molecule visits open channel states. Exact molecular determinants of such complex interactions of Iso with T-channel are currently not known, but further examination of T-channel kinetics in the presence of anesthetics could provide more details on the channel states and structures that Iso is able to affect. This could be accomplished through single-channel studies and more extensive molecular mutagenesis studies.

It is noteworthy that we identified several biophysical features of channel inhibition that may have a significant impact on active membrane firing that was observed previously with volatile anesthetic-induced inhibition of low-threshold calcium spikes in functional current-clamp recordings in intact thalamic slices (Ries and Puil, 1999; Joksovic et al., 2005b). For example, both voltage- and use-dependent inhibition, together with speeding of channel closure, will probably decrease the amount of calcium ions passing though the channel during action potentials. This in turn may profoundly affect the T-channel-dependent cellular excitability of these cells. It is important to mention that we and others have observed previously both voltage-dependent (Ries and Puil, 1999; Camara et al., 2001; Joksovic et al., 2005a) and voltage-independent (Takenoshita and Steinbach, 1991; Joksovic et al., 2005a) inhibition of different native T-currents by volatile anesthetics. It is not clear whether these inconsistencies are related to difference in recombinant versus native channels, different subunit composition, and/or different splice variants of T-channels present in native tissues. The last explanation seems plausible because all three

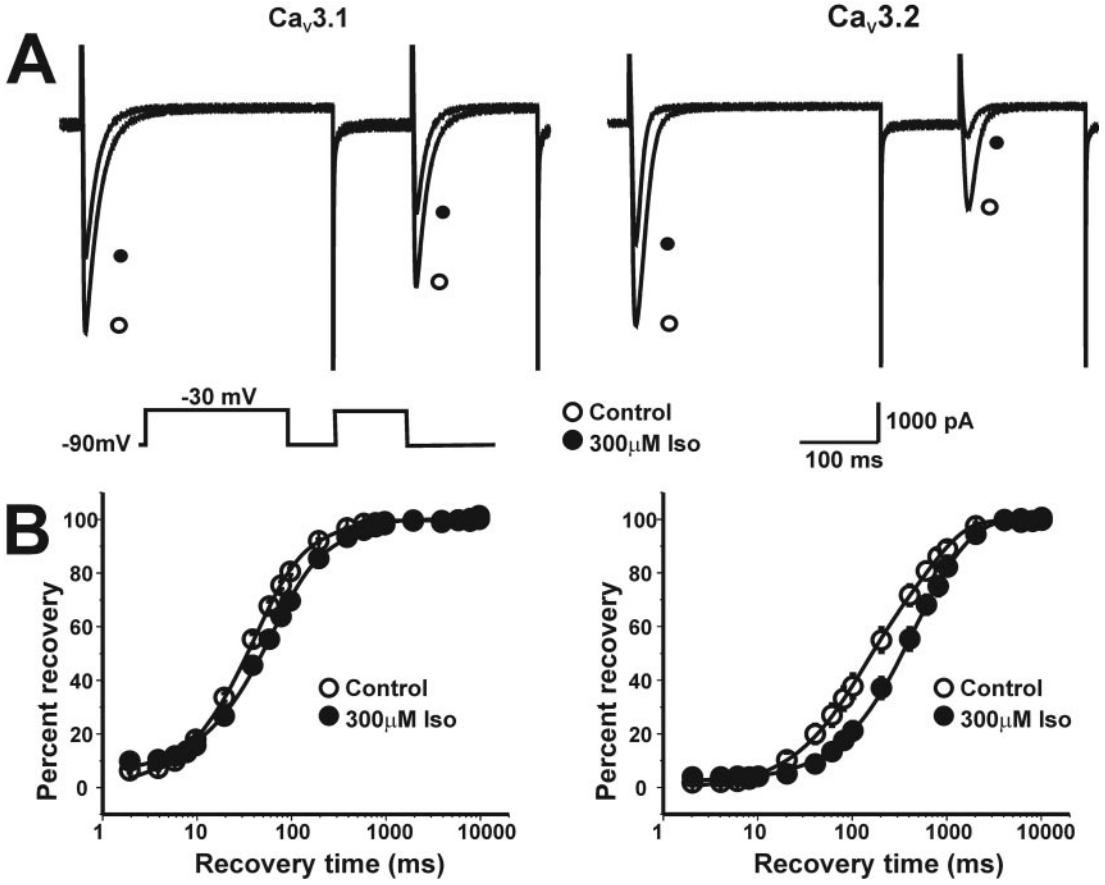

Fig. 6. Isoflurane slows recovery from inactivation of $Ca_V3.1$ (left) and $Ca_V3.2$ (right). A, traces from representative cells showing initial traces and traces after a 100-ms recovery interval in control conditions (open symbol) and after application of 300 μM Iso (filled symbol) in the same cells. Note that Iso diminished the current amplitude of the second pulse more than the first. Double-pulse protocol with variable recovery duration is depicted below. B, averaged data from multiple cells ($n = 5$) were fitted with a double exponential equation (solid lines): $Ca_V3.1$ (left) control: $\tau 1$, 216.4 ± 67.8 ms; $\tau 2$, 40.2 ± 3.3 ms; Iso: $\tau 1$, 384.0 ± 89.0 ms ($p < 0.01$); $\tau 2$, 60.5 ± 4.4 ms ($p < 0.01$); $Ca_V3.2$ (right) control: $\tau 1$, 580.2 ± 40.7 ms; $\tau 2$, 91.8 ± 8.2 ms; Iso: $\tau 1$, 893.0 ± 164.0 ms ($p < 0.01$); $\tau 2$, 292.6 ± 52.2 ($p < 0.01$).

T-channel isoforms may undergo extensive alternative splicing (Perez-Reyes, 2006).

Functional Considerations of T-Channel Inhibition by Isoflurane. T-channels are new arrivals in the field of anesthesia research, but the part they play in pain transmission and sleep pathway make them interesting targets for further exploration. Knockout (Choi et al., 2007) and knockdown studies (Bourinet et al., 2005) have firmly established a prominent role for T-channels in DRG in amplifying nociceptive signals in the periphery and possible contributors to the development of central sensitization in the dorsal horn (Ikeda et al., 2003). Based on these observations, it is not surprising that anesthetic agents that inhibit T-channels, such as Iso, also often possess notable analgesic qualities. In agreement with this, we report decreases in MAC requirements for Iso in $Ca_V3.2$ KO mice probably resulting from the prominent role of these channels in pain signaling. In contrast, studies of $Ca_V3.1$ KO mice did not find any changes in MAC for Iso or other volatile anesthetics (Petrenko et al., 2007). Although both $Ca_V3.1$ and $Ca_V3.2$ isoforms are simi-

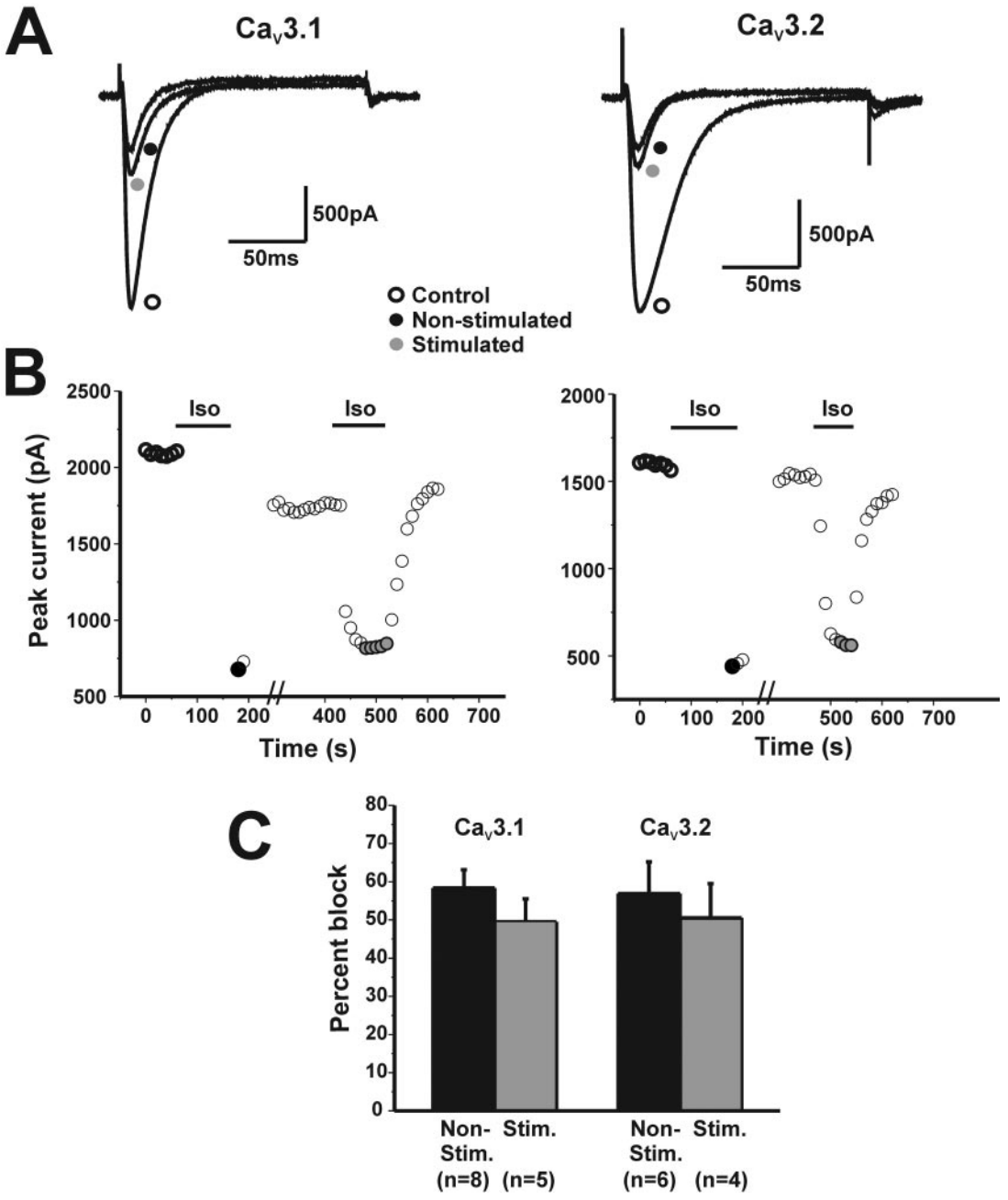

Fig. 7. Isoflurane inhibition of $Ca_V3.1$ and $Ca_V3.2$ during resting channel states. A, traces from representative cells transfected with $Ca_V3.1$ (left) or $Ca_V3.2$ (right) constructs (V_h −90 mV, V_t −30 mV). Control current is marked with an open symbol. Inhibition of current after application of 300 μM Iso during nonstimulated or resting states is shown using a black filled symbol, whereas constantly stimulated channel states are marked with a gray filled symbol. Bars indicate calibration. B, time courses of drug application of the same cells presented in A. Horizontal bars indicate times of application of 300 μM Iso. Note that maximal current inhibition was similar in both applications. C, pooled data compare the average block during the first pulse after nonstimulation with the drug (black bars) and after the drug effect reaches steady state (gray bars) during constant depolarizing pulses every 10 s. Percentage block: $Ca_V3.1$ nonstimulated, 58.3 ± 4.8; $Ca_V3.1$ stimulated, 49.5 ± 6.0 ($p > 0.05$); $Ca_V3.2$ nonstimulated, 56.9 ± 8.3; $Ca_V3.2$ stimulated, 50.5 ± 9.0 ($p > 0.05$). Error bars indicate S.E.M., and number of cells is indicated below each histogram bar.

larly inhibited by Iso, as shown in this study, and their mRNA transcripts are expressed in DRG and dorsal horn of the spinal cord (Talley et al., 1999), it seems that $Ca_V3.2$ is a more important contributor to anesthetic-induced analgesia. Our results strongly suggest that any future pharmaceutical developments of drugs that selectively inhibit $Ca_V3.2$ T-channels would be useful adjuvants for general anesthesia because they would reduce MAC.

We also found that genetic elimination of $Ca_V3.2$ leads to a marked delay of anesthetic induction with Iso. It is unlikely that this results from general depressant actions of Iso on the cardiovascular system because this effect was present only with lower concentrations of anesthetic. Thus, a specific role of $Ca_V3.2$ in neural pathways that mediate hypnotic/sedative effects of anesthesia is more likely. Although the role of $Ca_V3.2$ isoform in sleep is not established, $Ca_V3.1$ knockout mice also show slower anesthetic induction (Petrenko et al., 2007) and have an abnormal natural sleep phenotype, probably resulting from the lack of T-channels and underlying burst firing in the thalamic relay neurons (Lee et al., 2004; Anderson et al., 2005). Furthermore, recent studies implicate the thalamus as a possible central site for the hypnotic/

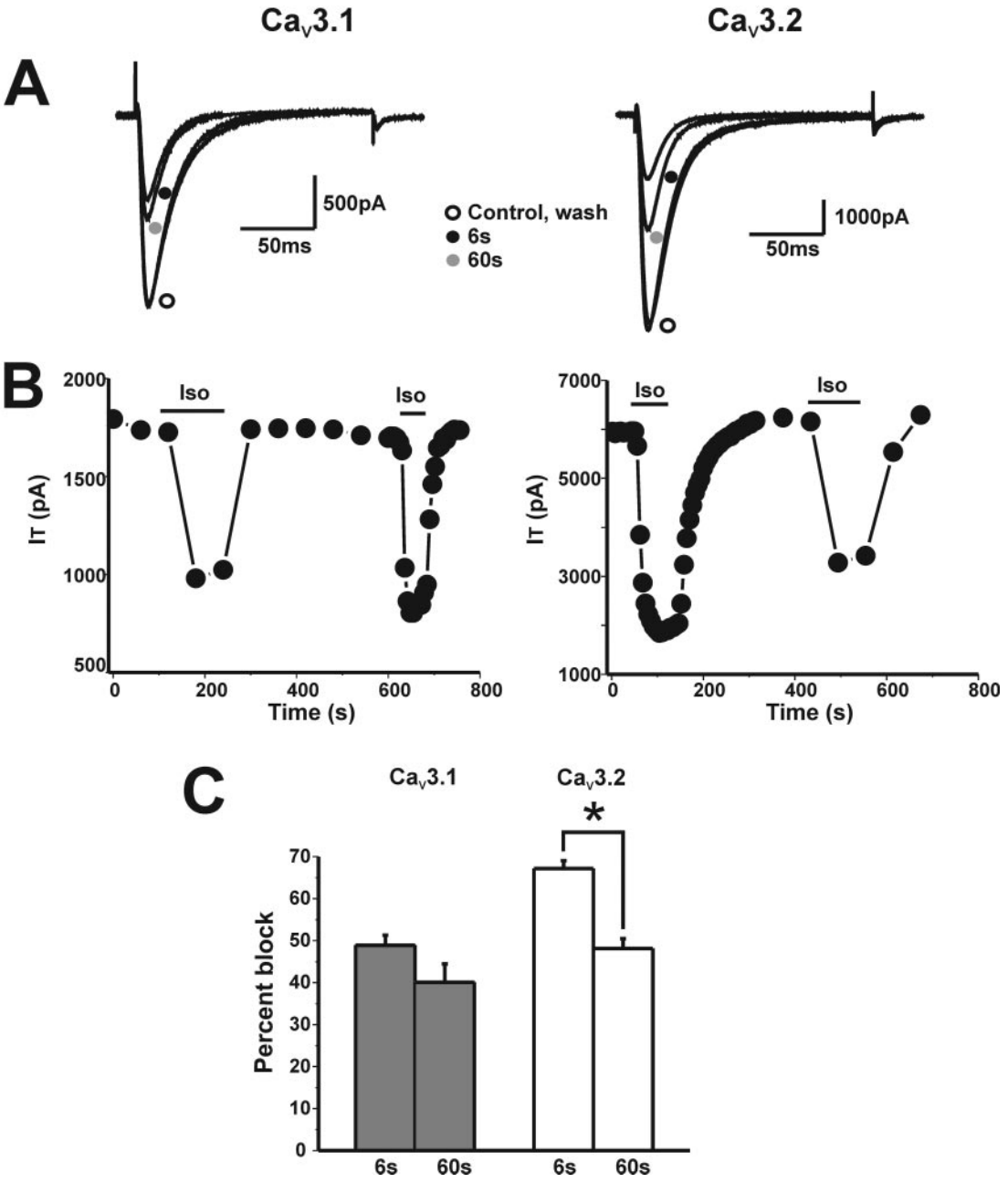

Fig. 8. Use-dependent block of $Ca_V3.1$ and $Ca_V3.2$ currents by isoflurane. A. traces from representative cells at V_h −90 mV in control conditions (open symbol) and before and during application of 300 μM Iso. Cells were stimulated with a depolarizing pulse to V_t −30 mV either every 6 s (black filled symbol) or every 60 s (gray filled symbol). B, time courses of Iso application (300 μM) in the same cells depicted in A. Horizontal bars indicate duration of application of Iso. Note that Iso inhibited more potently inhibits $Ca_V3.2$ currents with more frequent stimulation, whereas there is little difference in $Ca_V3.1$ current regardless of frequency of stimulation. C, pooled data (n = 7–8) show greater current inhibition of $Ca_V3.2$ but not $Ca_V3.1$ with Iso with more frequent membrane depolarization. Percentage block: $Ca_V3.1$ every 6 s, 48.9 ± 2.4; $Ca_V3.1$ every 60 s, 40.1 ± 4.4; $Ca_V3.2$ every 6 s, 67.2 ± 1.9; $Ca_V3.2$ every 60 s, 48.2 ± 2.3. *, significant difference, $p < 0.005$ with Student's t test.

sedative effects of many anesthetic agents. The thalamus is a major "gateway" of corticothalamocortical functional connections and expresses abundant Ca_V3 isoforms on neuronal somas and dendrites where these channels can shape neuronal excitability and synaptic integration, respectively. Functional imaging studies in both humans and animals have led to the theory that direct and indirect depression of thalamocortical neurons may provide a convergence point for neural pathways of anesthetic action, leading to a sleep-like state (Alkire et al., 2000). Mutually interconnected cortical, thalamic reticular neurons, and thalamic relay neurons exhibit tonic and burst firing that represent different functional modes (McCormick and Bal, 1997; Steriade, 2005). During tonic firing, which predominates during awake states, there is a faithful transfer of sensory information to cortical neurons. In contrast, during slow oscillations with a burst firing pattern, which critically depends on functional T-channels, there is an impairment of sensory transfer and transition to sleep states. It is well established that these slow oscillations underlie δ rhythms on electroencephalogram generated by the thalamocortical projection neurons and are very prominent during anesthesia (Franks, 2008) and in slow wave sleep (McCormick and Bal, 1997; Steriade, 2005). However, it is important to notice that Iso affects other ion channels in thalamocortical sensory pathways such as $GABA_A$ and potassium leak (I_{LEAK}) currents (Ries and Puil, 1999; Franks, 2008), and the overall effect of this anesthetic probably results from the interplay between all conductances that finely tune the inflow of sensory information into the thalamus.

Our findings of delayed anesthetic induction in $Ca_V3.2$ and similarly in $Ca_V3.1$ knockout mice (Petrenko et al., 2007) in vivo argue that at low and moderate levels of anesthesia with Iso (1.0–1.4% in vivo, or roughly 200–250 μM in vitro), T-channels are still functionally active and capable of producing burst firing in thalamocortical circuitries. This is probably because at subanesthetic concentrations, activation of

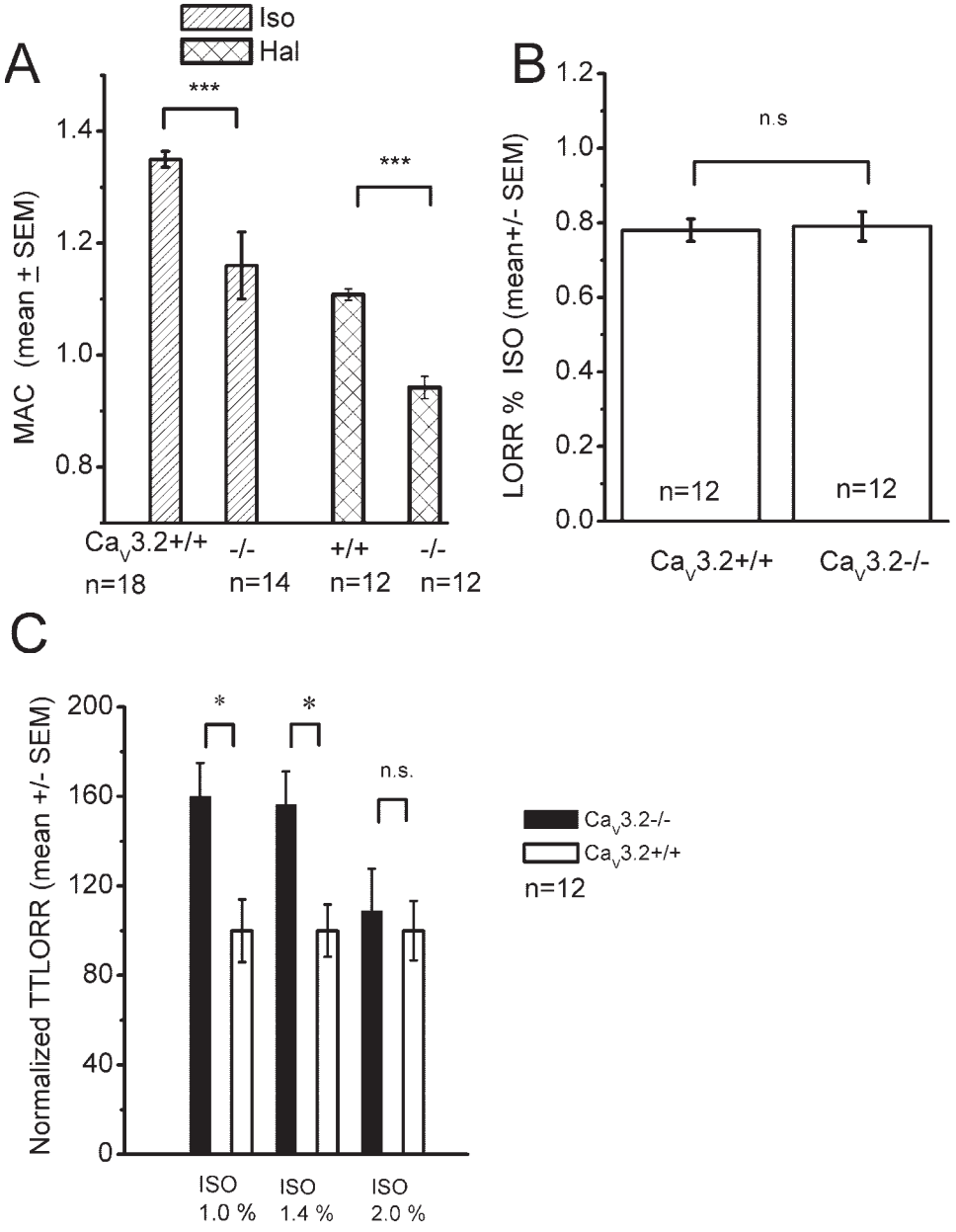

Fig. 9. $Ca_V3.2$ knockout mice have decreased MAC and slower onset of anesthetic induction than wild-type litter mates. A, histograms show decreased MAC measured by response to painful tail clamp to isoflurane and halothane. Error bars indicate S.E.M., and number of mice in each group is indicated below histogram bars. For isoflurane, MAC in WT mice was 1.35 ± 0.01% and in KO mice, 1.16 ± 0.06%. For halothane, MAC in WT mice was 1.10 ± 0.01% and in KO mice, 0.94 ± 0.02%. ***, $p < 0.001$ by Mann-Whitney rank sum test. B, histograms show no significant difference in LORR for isoflurane between wild-type mice [$Ca_V3.2(+/+)$] and knockout litter mates [$Ca_V3.2(-/-)$]. LORR in WT mice was 0.78 ± 0.03% and in KO mice, 0.79 ± 0.04% (n.s., not significant; $p > 0.05$ by t test). Number of experimental animals in each group is indicated in the bars. C, slower anesthetic induction with Iso in $Ca_V3.2$ KO mice (filled bars) than in wild-type litter mates (open bars) is indicated with longer normalized TTLORR at 1.0 and 1.4% inhaled gas but not at 2.0%. In each group, 12 animals were tested on different days with at least 1 week between experiments. Compared with wild-type group, KO mice had TTLOR increased by 60.0 ± 15.0% (1.0% Iso), 56.3 ± 15.0% (1.4% Iso), and by 8.8 ± 18.8% (2.0% Iso). *, significance at $p < 0.05$; n.s., not significant by t test.

$GABA_A$ receptors and I_{LEAK} would sufficiently hyperpolarize neurons, which would in turn deinactivate T-channels and relieve the state-dependent inhibition of thalamic T-channels by Iso. During deeper levels of anesthesia (e.g., 2% in vivo, roughly 400 μM in vitro), Iso causes a block of sensory information transfer between the thalamus and the cortex, with electroencephalogram patterns changing to a characteristic burst suppression mode and finally to an isoelectric line (Franks, 2008). This effect would be consistent with a strong direct inhibition of T-channels and more profound hyperpolarization of neuronal membrane. Both of these would lead to eventual cessation of the thalamocortical rhythmicity. Consistent with this, we did not find a difference in the speed of anesthetic induction with 2% Iso between $Ca_V3.2$ knockout mice and wild-type litter mates. In conclusion, the results of the present study support the idea that inhibition of neuronal T-channels in pain and sleep pathways by volatile anesthetics may contribute to useful clinical properties of these agents such as analgesia, immobility, and sedation/hypnosis.

Acknowledgments

We thank Dr. Edward Perez-Reyes for contributing stably transfected $Ca_V3.1$ and $Ca_V3.2$ HEK cell lines, Dr. Kevin Campbell for providing our initial pair of $Ca_V3.2$ KO mice, and Dr. Wenhao Xu for providing the services of the University of Virginia Gene Targeting and Transgenic Facility.

References

Alkire MT, Haier RJ, and Fallon JH (2000) Toward a unified theory of narcosis: brain imaging evidence for a thalamocortical switch as the neurophysiologic basis of anesthetic-induced unconsciousness. *Conscious Cogn* **9:**370–386.

Anderson MP, Mochizuki T, Xie J, Fischler W, Manger JP, Talley EM, Scammell TE, and Tonegawa S (2005) Thalamic Cav3.1 T-type Ca^{2+} channel plays a crucial role in stabilizing sleep. *Proc Natl Acad Sci U S A* **102:**1743–1748.

Bourinet E, Alloui A, Monteil A, Barrère C, Couette B, Poirot O, Pages A, McRory J, Snutch TP, Eschalier A, et al. (2005) Silencing of the $Ca_V3.2$ T-type calcium channel gene in sensory neurons demonstrates its major role in nociception. *EMBO J* **24:**315–324.

Camara AK, Begic Z, Kwok WM, and Bosnjak ZJ (2001) Differential modulation of the cardiac L- and T-type calcium channel currents by isoflurane. *Anesthesiology* **95:**515–524.

Choi S, Na HS, Kim J, Lee J, Lee S, Kim D, Park J, Chen CC, Campbell KP, and Shin HS (2007) Attenuated pain responses in mice lacking CaV3.2 T-type channels. *Genes Brain Behav* **6:**425–431.

Franks NP (2008) General anaesthesia: from molecular targets to neuronal pathways of sleep and arousal. *Nat Rev Neurosci* **9:**370–386.

Franks NP and Lieb WR (1994) Molecular and cellular mechanisms of general anaesthesia. *Nature* **367:**607–614.

Franks NP and Lieb WR (1982) Molecular mechanisms of general anesthesia. *Nature* **300:**487–493.

Herrington J and Lingle CJ (1992) Kinetic and pharmacological properties of low-voltage-activated Ca^{2+} current in rat clonal (GH3) pituitary cells. *J Neurophysiol* **68:**213–232.

Ikeda H, Heinke B, Ruscheweyh R, and Sandkühler J (2003) Synaptic plasticity in spinal lamina I projection neurons that mediate hyperalgesia. *Science* **299:**1237–1240.

Joksovic PM, Bayliss DA, and Todorovic SM (2005a) Different kinetic properties of two T-type currents of rat reticular thalamic neurones and their modulation by enflurane. *J Physiol* **566:**125–142.

Joksovic PM, Brimelow BC, Murbartián J, Perez-Reyes E, and Todorovic SM (2005b) Contrasting anesthetic sensitivities of slow T-type calcium channels of reticular thalamic neurons and recombinant $Ca_v3.3$ channels. *Br J Pharmacol* **144:**59–70.

Joksovic PM, Nelson MT, Jevtovic-Todorovic V, Patel MK, Perez-Reyes E, Campbell KP, Chen CC, and Todorovic SM (2006) $Ca_V3.2$ is the major molecular substrate for redox regulation of T-type Ca^{2+} channels in the rat and mouse thalamus. *J Physiol* **574:**415–430.

Lee J, Kim D, and Shin HS (2004) Lack of delta waves and sleep disturbances during non-rapid eye movement sleep in mice lacking α1G-subunit of T-type calcium channels. *Proc Natl Acad Sci U S A* **101:**18195–18199.

McCobb DP and Beam KG (1991) Action potential waveform voltage-clamp commands reveal striking differences in calcium entry via low and high voltage activated calcium channels. *Neuron* **7:**119–127.

McCormick DA and Bal T (1997) Sleep and arousal: thalamocortical mechanisms. *Annu Rev Neurosci* **20:**185–215.

McDowell TS, Pancrazio JJ, and Lynch C 3rd (1996) Volatile anesthetics reduce low-voltage-activated calcium currents in a thyroid C-cell line. *Anesthesiology* **85:**1167–1175.

Nelson MT, Joksovic PM, Perez-Reyes E, and Todorovic SM (2005) The endogenous redox agent L-cysteine induces T-type Ca^{2+} channel-dependent sensitization of a novel subpopulation of rat peripheral nociceptors. *J Neurosci* **25:**8766–8775.

Perez-Reyes E (2006) Molecular characterization of T-type calcium channels. *Cell Calcium* **40:**89–96.

Perez-Reyes E (2003) Molecular physiology of low-voltage-activated T-type calcium channels. *Physiol Rev* **83:**117–161.

Petrenko AB, Tsujita M, Kohno T, Sakimura K, and Baba H (2007) Mutation of alpha1G T-type calcium channels in mice do not change the anesthetic requirements for loss of righting reflex and minimum alveolar concentration but delays the onset of anesthetic induction. *Anesthesiology* **106:**1177–1185.

Rampil IJ (1994) Anesthetic potency is not altered after hypothermic spinal cord transection in rats. *Anesthesiology* **80:**606–610.

Ries CR and Puil E (1999) Mechanisms of anesthesia revealed by shunting actions of isoflurane on thalamocortical neurons. *J Neurophysiol* **81:**1795–1801.

Rudolph U and Antkowiak B (2004) Molecular and neuronal substrates for general anaesthetics. *Nat Rev Neurosci* **5:**709–720.

Steriade M (2005) Sleep, epilepsy and thalamic reticular inhibitory neurons. *Trends Neurosci* **28:**317–324.

Study RE (1994) Isoflurane inhibits multiple voltage-gated calcium current in hippocampal pyramidal neurons. *Anesthesiology* **81:**104–116.

Takenoshita M and Steinbach JH (1991) Halothane blocks low-voltage-activated calcium current in rat sensory neurons. *J Neurosci* **11:**1404–1412.

Talley EM, Cribbs LL, Lee JH, Daud A, Perez-Reyes E, and Bayliss DA (1999) Differential distribution of three members of a gene family encoding low voltage-activated (T-type) calcium channels. *J Neurosci* **19:**1895–1911.

Todorovic SM, Jevtovic-Todorovic V, Meyenburg A, Mennerick S, Perez-Reyes E, Romano C, Olney JW, and Zorumski CF (2001) Redox modulation of T-type calcium channels in rat peripheral nociceptors. *Neuron* **31:**75–85.

Todorovic SM and Lingle CJ (1998) Pharmacological properties of T-type Ca^{2+} current in adult rat sensory neurons: effects of anticonvulsant and anesthetic agents. *J Neurophysiol* **79:**240–252.

Todorovic SM, Perez-Reyes E, and Lingle CJ (2000) Anticonvulsants but not general anesthetics have differential blocking effects on different T-type current variants. *Mol Pharmacol* **58:**98–108.

Urban BW (2002) Current assessment of targets and theories of anaesthesia. *Br J Anaesth* **89:**167–183.

Address correspondence to: Dr. Slobodan M. Todorovic, Department of Anesthesiology, University of Virginia Health System, Mail Box 800710, Charlottesville, VA 22908-0710. E-mail:st9d@virginia.edu